Phonon modes and Raman scattering in Si$_x$Ge$_{1-x}$ nanocrystals: microscopic modelling

A. S. Vasin[1], O. V. Vikhrova[1], and M. I. Vasilevskiy[*,2]

[1] Department of Physics and NIFTI, N. I. Lobachevskii University, Nizhnii Novgorod 603600, Russia
[2] Centro de Física, Universidade do Minho, Campus de Gualtar, 4710-057 Braga, Portugal

* Corresponding author: e-mail mikhail@fisica.uminho.pt,Phone: +351 253604 069, Fax: +351 253604 061

Si$_{1-x}$Ge$_x$nanocrystals (NCs) of different composition and size were generated using the Molecular Dynamics (MD) method by minimizing NC's total energy calculated using Tersoff's empirical potential and applying rigid boundary conditions. The dynamical matrix of the relaxed NC was constructed and the NC phonon modes were calculated. The localisation of the principal (Si-Si, Si-Ge and Ge-Ge) modes is investigated by analysing their inverse participation ratio. The dependence of the corresponding Raman spectra, obtained by employing the bond polarisability model, upon x and the NC size is presented and compared to previous calculated results and available experimental data.

1 Introduction One of the promising ways to achieve direct band gap structure in silicon and its alloys with the germanium is to use the 3D quantum confinement effect characteristic of semiconductor quantum dots (QDs). Beyond self-assembled QDs [1], Si-Ge alloy nanocrystals (NCs), either embedded in SiO$_2$ matrix [2-4] or freestanding [5], have been obtained and studied, showing size-dependent optical spectra.

Raman spectroscopy, a method of choice to investigate nanomaterials, was used in all these works on Si-Ge NCs, as well as it was applied to study Si$_x$Ge$_{1-x}$ alloys in bulk [6] and epitaxial thin film [7] forms.In all cases, the spectra are characterised by three dominant peaks centred near 300, 400 and 500 cm^{-1}, associated with optical phonons involving Ge-Ge, Si-Ge, and Si-Si stretching motions, respectively [6]. However, the precise positions and the amplitudes of these peaks depend on several factors, such as crystal lattice relaxation, alloy composition and details of atomic distribution over the lattice (correlations) and, in the case of NCs, size effect. For their correct interpretation, theoretical and computational work is required.

Several computational works have been performed so far, devoted to the calculation of phonon properties and Raman spectra of Si$_{1-x}$Ge$_x$alloys [6-12]. Because of the absence of translational symmetry, the use of more accurate *ab initio* models is limited to small NCs [8-10], while empirical potential models used in [6, 7, 11, 12] can be applied to larger systems and still can provide quite a good agreement with experimental data.
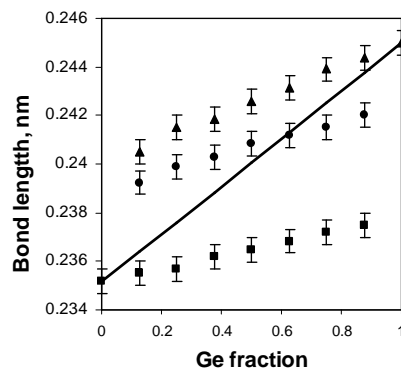
Figure 1 Calculated variation of bond lengths with Ge fraction in relaxed Si$_x$Ge$_{1-x}$NCs: Si-Si (squares), Si-Ge(circles), andGe-Ge(triangles) bonds. Straight line corresponds to Vegard's law.

However, probably the most popular empirical potential-scheme, the valence force field (VFF) model, relies on Vegard's law (i.e. linear variation of the lattice constant with composition) when applied to random alloys [11, 12], whereas it is known that the bond length distribution in Si-Ge alloys is trimodal and only the average of the three types of bonds follows the Vegard's law [13].

In this work, we calculate the phonon properties, namely, the density of states (DS) and the inverse participation ratio (IPR), as well as the Raman scattering spectra of Si_xGe_{1-x} crystallites of different composition and size by using a three-particle empirical potential proposed by Tersoff [14]. Its advantage in comparison with the VFF model is that it can be used for relaxing the NC to thermodynamical equilibrium (for a given composition) before considering the lattice dynamics.

2 Relaxed Si-Ge NCs

2.1 NC building algorithm Crystallites consisting of up to N=1647 atoms were built by randomly distributing some xNGe and (1-xN) Si atoms over the sites of a diamond lattice, starting from a central atom and filling its 1-st, 2-nd, … coordination shells. Initially, the lattice constant was chosen according to Vegard's law. This way we obtained "nearly spherical" crystallites of $O_h$symmetry.

Interactions between the atoms were defined according to the Tersoff potential [14]. Relaxation to the minimum of the total energy of the crystallite was achieved by allowing the atoms to move in response to the forces produced by their neighbours. Having in mind NCs embedded in a matrix, rigid boundary conditions were applied, which means that the positions of the atoms in two outer shells were fixed although they were considered interacting with the (movable) atoms in the interior shells. By using the MD method (Verlet algorithm [15]) with integration of the equations of motion at each temporal step (not exceeding 10^{-15} s) we obtained equilibrium crystallites that no longer possessed the O_h symmetry (except for $x = 0$ or 1).

2.2 Bond length distribution The variation of the average bond lengths, for Si-Si, Si-Ge and Ge-Ge bonds, with alloy composition is shown in Fig. 1. The dependence on x is rather weak for the three types of bonds. It is in agreement with the idea that the relaxation of the microscopic strain related to the difference between the bond lengths in pure Si and Ge, occurs mostly via distortion of the bond angles and to a lesser extent by changing the bond lengths [13]. The relative contribution of these two mechanisms of strain relaxation can be quantified in terms of so called topological rigidity parameter (a^{**}) [13, 16]. When a^{**} =1, the lattice is flexible, i.e. every bond adjusts to its natural length (so called Pauling limit), while a^{**} =0 corresponds to a perfectly rigid lattice, so that all bonds adjust their lengths to a common value [13]. Our calculations yield a^{**}=0.73, 0.64 and 0.50 for Si-Si, Si-Ge and Ge-Ge bonds, respectively. These values are close to those obtained in the *ab initio* study [16] where the bulk alloy was

modelled by applying periodical boundary conditions. We can conclude that in $Si_{1-x}Ge_x$NCs, likewise in the bulk alloy, bond lengths depend on composition much weaker than prescribed by Vegard's law and that these variations are type specific.

3 Lattice dynamics and Raman spectra

3.1 Phonon DS and IPR The phonon modes of the generated NCs were calculated by finding the eigenstates of the dynamical matrix whose elements were obtained by differentiating theTersoff potential with respect to atomic coordinates. The density of states versus frequency was calculated as a sum of Lorentzian functions (with a homogeneous broadening of 10 cm^{-1}) centred at each eigenfrequency. Figure 2 presents the total DS averaged over a number of samples for each composition. These results correspond to the largest crystallites studied (12 atomic shells).

In general, the shape of the phonon DS obtained in our calculations is similar to the previously calculated data for SixGe1-x alloy NCs [11, 12]. In the optical phonon range (ω/ω_{max}> 0.5) we clearly see three bands corresponding to the experimentally observed Raman scattering peaks (ω/ω_{max}= 0.6, 0.8 and 1), well known for the bulk alloy. The feature at ω/ω_{max}= 0.15 corresponds to the Brillouin zone edge TA phonons of germanium ($\approx$ 80 cm^{-1}). Some of the smaller features in the middle of the spectrum can be associated with surface vibrations but we have not been able to doubtlessly identify them.
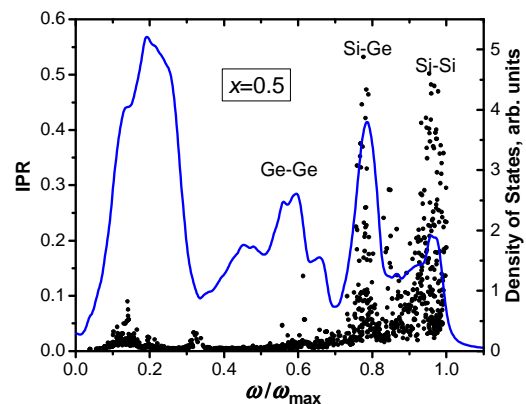

Figure 2(colour online) Phonon DS calculated for $Si_{0.5}Ge_{0.5}$NC, averaged over several NC configurations (full curve), and IPR of vibrational modes for a single NC configuration, plotted against their frequencies (points).

In order to investigate the localisation of some characteristic modes, we calculated their inverse participation ratio, IPR = $\Sigma_j(\mathbf{u}_j)^4$, where **u**is the normalised eigenvector of the considered mode and the sum runs over all lattice sites. Large IPR values are characteristic of strongly localized modes with only few atoms vibrating [17]. As expected,

the optical phonon modes are stronger localised than acoustical vibrations (see Fig. 2). IPR results obtained for other Ge contents (not shown) indicate that the Si-Si mode becomes much less localised for $x < 0.3$, as does the Ge-Ge mode for $x > 0.7$. On the contrary, the Si-Ge mode always remains strongly localised. By analysing the corresponding eigenvectors, we established that the DS peak designated "Si-Ge mode" ($\omega/\omega_{max} \approx 0.8$) is associated with vibrations of Si atoms surrounded by 3 or 4 almost motionless Ge atoms.

3.2 Raman spectra Non-resonant Raman spectra were calculated within the bond polarisability model [18]. Assuming that the deviations from the perfect tetrahedric bonding are small in our relaxed NCs, only the α_1 term was taken into account since the other two vanish for a perfect diamond lattice. The unpolarised Raman scattering intensity spectra, averaged over several NC configurations (with the same size and composition) and normalised by the NC volume, are shown in Fig. 3.
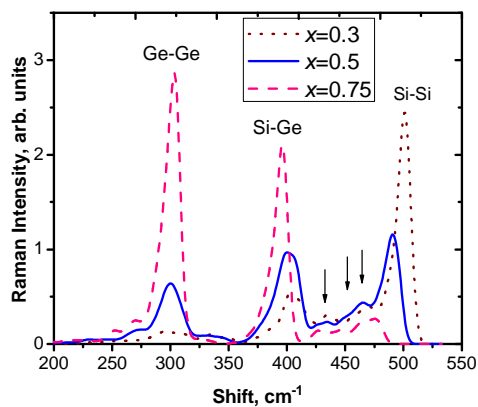
Figure 3 (colour online) Raman spectra of $Si_{1-x}Ge_x$ NCs of three different compositions. NC size 3.9 nm. Minor features are marked by arrows.

The spectra of Fig. 3 are in qualitative agreement with both previously calculated [11, 12] and experimental [2-4, 8] results. The shape of the spectra is determined by both small size (confinement) and alloy disorder effects. The size effect is clearly seen in Fig. 4 for $x=0$. The phonon confinement moves the Si-Si Raman peak downwards, with the shift with respect to bulk peak position scaling approximately as D^{-2} with the NC size (D), in agreement with the macroscopic model predictions [19] and experimental data [2]. The existence of the phonon confinement effect in alloy NCs means that the fundamental (Si-Si and Ge-Ge) modes are sufficiently delocalised, at least in a certain range of x [20].

The dependence of the positions and heights of the main Raman peaks upon the alloy composition qualitatively follows the trends known for bulk $Si_{1-x}Ge_x$ alloys and relaxed epilayers [6, 7, 10]. As expected, the Ge-Ge mode grows in intensity and becomes narrower with the increase of Ge contents. For the Si-Si mode, the tendency is the opposite. The spectral positions of the Ge-Ge and Si-Si modes for different x can be approximated quite well by linear functions. For the latter, our results practically coincide with the previously published data [7, 10], while for the Ge-Ge mode we found

$$\omega_{Ge-Ge} = 298 + 6.6x \quad [\text{cm}^{-1}], \tag{1}$$

which is weaker than obtained for relaxed $Si_{1-x}Ge_x$ epilayers [7]. It should be pointed out that we could clearly identify this mode in our spectra only for $x > 0.2$, even for the largest NC size, which can be the cause for the discrepancy.
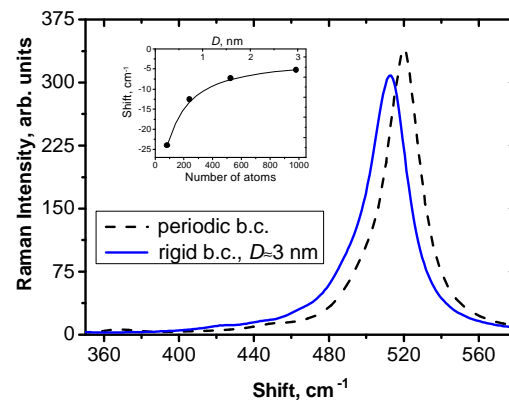
Figure 4 (colour online) Raman spectrum of silicon calculated with rigid (NC) and periodic (c-Si) boundary conditions. Inset shows the position of the peak *versus* size for silicon NCs ($x=0$).

The Si-Ge mode also becomes noticeable only for $x \gtrsim 0.2$. Its intensity reaches a maximum at $x \approx 0.75$ and then decreases and vanishes. So, our results do not confirm the intuitive idea that it should be simply proportional to the fraction of Si-Ge bonds, $2x(1-x)$, as it has been suggested by some authors [3]. The spectral position of the Si-Ge band peak *versus* x can be approximated by a quadratic polynomial,

$$\omega_{Si-Ge} = 400 + 34.2x - 50.2x^2 \quad [\text{cm}^{-1}]. \tag{2}$$

It converges to the Si local vibrational mode (385 cm^{-1} [10]) in the limit $x \to 1$. However, it should be noted that, in general, the Si-Ge band probably is composed of *two* peaks, as can be seen also in Fig. 2 and has been reported in some previous studies [7].

Smaller features that are clearly seen in the NC Raman spectra have also been observed in previous studies, both experimental and computational, of bulk crystals and relaxed epilayers of $Si_{1-x}Ge_x$ alloys, and their assignment has attracted considerable attention (see [10] and references therein). The three minor peaks marked by arrows in Fig, 3

were observed by Alonso and Winer [6], together with the three major peaks giving rise to a "six-oscillator model" [1×(Ge-Ge), 1×(Si-Ge), 4×(Si-Si)] of the Si_xGe_{1-x} Raman pattern. In the recent work [10], it was suggested to consider 7 oscillators, [1 × (Ge-Ge), 4 × (Si-Ge), 2 × (Si-Si)]. As far as experiments performed on Si_xGe_{1-x} NCs are concerned, only *one* minor mode (at ≈ 430 cm^{-1}) has been observed so far [4], while e.g. Raman spectra of self-assembled Si_xGe_{1-x} QDs presented in [21] are clearly free from any extra features. We plan a more detailed study of the minor Raman features and the Si-Ge band fine structure in the future.

4 Conclusions We have shown the potential of our approach using three-particle empirical potentials for modelling the lattice dynamics of Si_xGe_{1-x} NCs. It has some advantages in comparison with both the *ab initio* density functional theory approach (the possibility of considering larger crystallites) and the popular empirical VFF model (the incorporation of relaxation to equilibrium structure leading to the realistic trimodal distribution of bond lengths).

By considering crystallites with rigid boundary conditions, we modelled NCs embedded in a matrix (e.g. SiO_2). We found that the quantum confinement effect is present for the fundamental (Si-Si and Ge-Ge) modes, consisting in a red shift of the mode frequencies in NCs with very small size. The intermediate (Si-Ge) mode is shown to be related to the vibrations of solitary Si atoms surrounded by 3 or 4 almost motionless Ge atoms. These vibrations are strongly localised and should be less influenced by the quantum confinement effect.

References

[1] A. Malachias, S. Kycia, G. Medeiros-Ribeiro, R. Magalhães-Paniago, T. I. Kamins, and R. S. Williams, Phys. Rev. Lett. **91**, 176101 (2003).

[2] S. Takeoka, K. Toshikiyo, M. Fujii, S. Hayashi, and K. Yamamoto, Phys. Rev. B **61**, 15988 (2000).

[3] N. A. P. Mogaddam, A.S.Alagoz, S.Yerci, R.Turan, S.Foss, and T.G.Finstad, J. Appl. Phys. **104**,134309 (2008).

[4] L. Z. Liu, X. L. Wu, J. S. Shen, T. H. Li, F. Gao, and P. K. Chu, Chem. Commun. **46**, (2010) 5539.

[5] X. D. Pi and U. Kortshagen, Nanotechnology **20**, 295602 (2009).

[6] M. I. Alonso and K. Winer, Phys. Rev. B **39**, 10056 (1989).

[7] V. A. Volodin, M. D. Efremov, A. S. Deryabin, and L. V. Sokolov, Semiconductors **40**, 1314 (2006).

[8] L. Z. Liu, X. L. Wu, Y. M. Yang, T. H. Li, and P. K. Chu, Appl. Phys. A **103**, 361 (2011).

[9] M. A. Abdulsattar, J. Appl. Phys. **111**, 044306 (2012).

[10] O. Pagès, J. Souhabi, V. J. B. Torres, A. V. Postnikov, and K. C. Rustagi, Phys. Rev. B **86**, 045201 (2012).

[11] S.-F. Ren, W. Cheng, and P. Y. Yu, Phys. Rev. B.**69**, 235327(2004).

[12] W. Cheng, D. Marx, and S.-F.Ren, Front. Phys. China **3**, 165 (2008).

[13] C. Tzoumanekas and P. C. Kelires, Phys. Rev. B **66**, 195209 (2002).

[14] J. Tersoff, Phys. Rev. B **39**, 5566 (1988).

[15] L. Verlet, Phys. Rev. **159**, 98 (1967).

[16] P. Venezuela, G. M. Dalpian, and J. R. da Silva, Phys. Rev. B **64**, 193202 (2001).

[17] M. I. Vasilevskiy, O. V. Vikhrova, and S. N. Ershov, Phys. Solid State **45**, 1154 (2003).

[18] R. Alben, D. Weaire, J. E. Smith, and M. H. Brodsky, Phys. Rev. B **11**, 2271 (1975).

[19] A. G. Rolo and M. I.Vasilevskiy, J. Raman Spectrosc. **38**, 618 (2007).

[20] E. S. FreitasNeto, S. W. da Silva, P. C. Morais, M. I. Vasilevskiy, M. A. Pereira-da-Silva, and N. O. Dantas, J. Raman Spectrosc. **42**, 1660 (2011).

[21] V. O. Yakhimchuk*et.al.*, Semiconductor Physics, Quantum Electronics & Optoelectronics **7**, 456 (2004).